ACS OMEGA

Article

Cite This: ACS Omega 2019, 4, 15849−15855

http://pubs.acs.org/journal/acsodf

Catalytic Deoxygenation of the Oil and Biodiesel of Licuri (*Syagrus coronata*) To Obtain *n*-Alkanes with Chains in the Range of Biojet Fuels

Pedro H. M. Araújo,[†,‡] Ary S. Maia,[†] Angela M. T. M. Cordeiro,[‡,§] Amanda D. Gondim,[∥] and Nataly A. Santos*[,†,‡,§]

[†]Programa de Pós-Graduação em Química, CCEN, [‡]Laboratório de Tecnologia de Biocombustíveis, IDEP, and [§]Departamento de Tecnologia de Alimentos, Universidade Federal da Paraíba (UFPB), 58051900 João Pessoa, Brazil

[∥]Instituto de Química, Universidade Federal do Rio Grande do Norte (UFRN), 59072970 Natal, Brazil

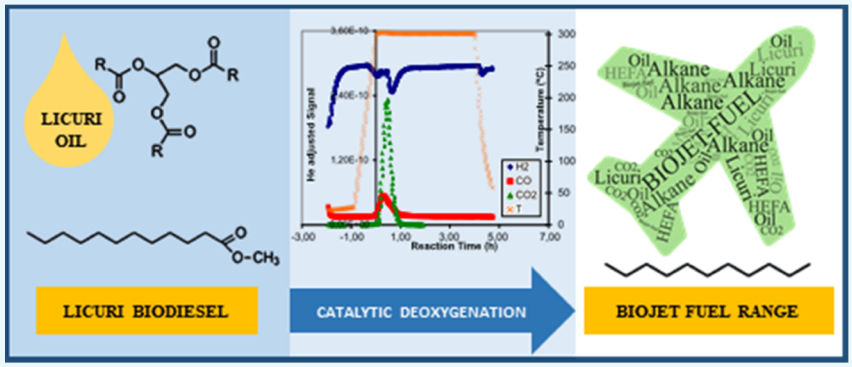

ABSTRACT: Aviation industry has the challenge of halving CO_2 emissions by 2050, as compared to 2005. An alternative are drop-in biofuels, which are sustainable and fully compatible with aircraft engines and also can be mixed with fossil jet fuel. Among the feedstock for biojet fuel production, licuri (*Syagrus coronata*) can be highlighted as most of its fatty acids are in the jet fuel range. Thereby, this work investigated the composition and physicochemical characterization of licuri oil and licuri biodiesel, both with satisfactory results according to international standards, with the purpose of obtaining hydrocarbons in the range of jet fuel from these feedstock, by catalytic deoxygenation. The semi-batch reaction, using a 5% Pd/C catalyst at 300 °C and 207 psi, produced *n*-alkanes with a conversion of up to 39.2%. The *n*-alkane selectivity was 80.7%, in addition to CO_2 selectivity of 83.4% for biodiesel, indicating the preference for the decarboxylation pathway and also confirming licuri as a potential raw material for biojet fuel.

1. INTRODUCTION

One of the main goals of the aviation industry is to develop an effective solution for its environmental impact and ensure the sustainability of the growth of this means of transport, what induces economic growth. CO_2 emissions from this sector were 705 million tons in 2013. This number accounted for about 2% of global emissions in that year and, if nothing is done, it should increase by 340% to 3.1 billion tons by 2050. The challenge, therefore, is to halve CO_2 emissions by 2050, as compared to the 2005 values. Thus, the aviation industry would become carbon-neutral by 2020, as established by the International Air Transport Association.[1−3]

The aviation industry understands that to meet the goal of reducing CO_2 emissions, it is necessary to replace part of the fossil fuel used with biofuel. Two conventional options are biodiesel and ethanol, which are widely produced and sold renewable fuels. However, they are chemically distinct from fossil fuels and cannot be considered as substitutes for all petroleum-derived fuels.[4] Therefore, this industry seeks the development of drop-in biofuels, which are fully compatible with current technologies and can be mixed in proportions up to 50% v/v. with fossil jet fuel, without the need for changes in the engines, aircraft, and distribution infrastructure. One of its advantages is its use without compromising the safety of the aviation system.[5−7]

These drop-in fuels are very similar in performance to the conventional jet fuel and they are virtually free of sulfur and aromatics.[8] In addition, the synthetic fuels have excellent properties once they do not present oxygen in their composition.[9]

There are several methods for processing raw material into biojet fuel. Among them, two stand out, as they are certified and standardized by ASTM in a mixture of up to 50% for use in jet fuel: Fischer−Tropsch (FT-SPK) and hydroprocessed esters and fatty acids (HEFA-SPK). There is also the alcohol to jet (ATJ-SPK) and hydroprocessed fermented sugars (HFS-

Received: June 12, 2019
Accepted: August 14, 2019
Published: September 19, 2019

DOI: 10.1021/acsomega.9b01737
ACS Omega 2019, 4, 15849−15855

SIP), also standardized, but only allowed for smaller proportions in the mixtures.[10,11]

Alternative routes for jet fuel production change according to the feedstock used in the synthesis. Jet fuel synthesized from renewable oils can be defined as hydroprocessed renewable jet, also known as hydroprocessed esters and fatty acids (HEFA) or paraffin synthetic kerosene (bio-SPK).[2] Biojet fuels differ from renewable diesel by composition. Renewable diesel contains C10−C22 hydrocarbons, and biojet fuel is composed of a mixture of C8−C16 with a maximum aromatic content of 25%, with a very low freezing point. The hydrotreating process of fatty acids allows for the production of hydrocarbons from a renewable source, which can be processed into aviation fuels, as well as conventional transport fuels, such as biogasoline and renewable diesel. However, jet fuel needs to be completely dry, and it needs to display a much lower freezing point and a smaller viscosity than other fuels to meet the requirements of the international standard ASTM D 1655. The main composition difference between jet fuel and diesel is the hydrogen chain size range. Diesel oil has a higher hydrocarbon chain size than jet fuel.[12]

In the hydrotreating process, deoxygenation occurs, which leads to the formation of saturated and/or unsaturated linear hydrocarbons by two main reaction routes: decarboxylation (eq 1), generating paraffinic hydrocarbons, and decarbonylation (eq 2), which produces olefins.[13] A third route is also possible to occur, on a smaller scale: hydrodeoxygenation (eq 3), in which there is no carbon loss in the chain.[14] Snåre et al.[15] observed that, for stearic acid, both the decarbolylation and decarbonylation reactions are thermodynamically favorable

$$R{-}CH_2{-}COOH \rightarrow R{-}CH_3 + CO_2 \quad (1)$$

$$R{-}CH_2{-}COOH \rightarrow R{=}CH_2 + CO + H_2O \quad (2)$$

$$R{-}CH_2{-}COOH + 3H_2 \rightarrow R{-}CH_2{-}CH_3 + 2H_2O \quad (3)$$

The principle of the catalytic deoxygenation reaction is based on the cracking of the fatty acids at the conditions of high temperatures and pressure, with the aid of the catalyst. As a result, according to eqs 1−3, paraffinic and olefinic hydrocarbons are generated as the main products. Carbon dioxide (CO_2), which is one of the main gaseous products formed, helps to maintain a high catalytic activity in the reactor because it is more easily desorbed than carbon monoxide (CO), and the consumption of hydrogen (H_2) decreases once the hydrogen products formed from eq 1 are saturated.[16−18]

Simakova et al.[18] studied the decarboxylation rates of different fatty acids, whose chains varied between 18 and 22 carbons. The results were almost similar upon the usage of the Pd/C catalyst, regardless the fatty acid chain size.

Mäki-Arvela et al.[19] reported rather comprehensive investigations on the deoxygenation of fatty acids in the liquid phase for the biofuel production. The catalyst used in the catalytic deoxygenation at 300 °C included Ir, Ni, Pt, Rh, and Ru on different supports; Ni-Raney, PdPt/C, and Os/C; and 1, 5, and 10% by weight Pd/C. The 5% Pd/C catalyst was identified as the most active and most selective one for *n*-heptadecane production through the deoxygenation of stearic acid.[20]

Choi et al.[7] obtained yields above 86% for the catalytic deoxygenation reaction. In this study, it was possible to obtain alkanes in the range of biojet fuel without the addition of hydrogen. A catalyst based on W/Pt/TiO_2 was prepared and used in the catalytic deoxygenation of fatty acids without added hydrogen, and it was possible to obtain products free of oxygen, which can be transformed into biojet fuel.

The precursor substrates of the methyl or ethyl esters, whose paraffinic chain size resembles the one of the range of petroleum distillates equivalent to fossil jet fuel, comprises fractions of vegetable oils or animal fats with linear or branched chains containing 10−17 carbons.[16] For this reason, several studies and flight tests have been carried out with biojet fuel obtained from babassu and coconut, which display as major compounds lauric acid (C12:0), and palm whose principal component is palmitic acid (C16:0). So, another oleaginous that deserves attention is licuri (*Syagrus coronata*). The fatty acid with the highest concentration in licuri oil is lauric acid (C12:0).[21] Therefore, licuri is shown as a possible feedstock source for the production of biojet fuel.

Licuri is the fruit of a Brazilian native palm from Braziian Atlantic Forest, it is also adjusted to drier regions, and it has a great energetic potential. The species stands out because it has adapted very well to the semiarid region of northeastern Brazil, which presents low social and economic development rates. Licuri palm, whose almond possesses a high oil content (around 38 wt %), presents high potential for the development of this region, with an annual oil production of 99 million tons. It has many utilities, from biofuels production to medicinal, building, and handcrafting applications. In addition, it has a high production capacity, equivalent to 4 t ha^{-1} per year of almonds, as this palm tree blooms and fruits the whole year.[21,22]

Therefore, the present work aimed at obtaining hydrocarbons between C9 and C17, in the range of biojet fuel, originating from licuri oil and licuri biodiesel. They were subjected to catalytic deoxygenation by semi-batch reaction, using the Pd/C catalyst.

2. EXPERIMENTAL SECTION

2.1. Licuri Oil. Licuri oil was analyzed by a model GCMS-QP2010 Shimadzu gas chromatograph coupled to the mass spectrometer (GC-MS), equipped with split injector, for identification of its components. The capillary column used was a Durabond-DB-5HT (Agilent Technologies; length, 30 m; diameter, 25 mm; film thickness, 0.25 μm). Helium was used as carrier gas at a flow rate of 3 mL min^{-1}, and the sample injection volume was 1 μL. The MS detector temperature was 250 °C. The oil was esterified following the methodology described by Hartman and Lago.[23] In addition to its composition, the oil was also evaluated by its physicochemical characterization. The acid value was determined by the Ca 5a-40 method and the iodine value according to the Cd 1-25 method.[24] The density at 20 °C was performed on a KEM-DA130N portable digital densimeter, following the ASTM standard D 4052. The flow properties assessed were kinematic viscosity, cloud point, pour point, and cold filter plugging point. The kinematic viscosity was measured at 40 °C, according to the ASTM standard D 445 in a Julabo-V18 bath viscosimeter. The cloud point and the pour point were performed in a model MPC-102L Tanaka Pour/Cloud Point Tester, according to the standards ASTM D 7683 and ASTM D 6749, respectively. The cold filter plugging point was determined in a model AFP-102 performed on Tanaka, according to ASTM D 6371. The oxidation stability analysis was carried out in a model 743 Rancimat (Metrohm), according to AOCS Cd 12B.

DOI: 10.1021/acsomega.9b01737
ACS Omega 2019, 4, 15849−15855

2.2. Licuri Biodiesel Synthesis and Characterization. The transesterification was performed by the methyl route, with basic catalysis, in a 1:6 molar ratio (oil/methanol). The catalyst used was potassium hydroxide (97% purity, Fisher Chemical) and methanol (99.8% purity, Fisher Chemical). Licuri oil, extracted in the state of Bahia, Brazil, was added to the alkoxy, and the mixture was stirred for 40 min, at 30 °C. Glycerin was removed by decantation. The biodiesel was washed with heated water at 60 °C until the catalyst was completely removed. Subsequently, vacuum drying was carried out at 80 °C. The ester content was determined by gas chromatography following the method EN 14103.[25]

The parameters acid value and iodine value were determined in a Metrohm potentiometric titrator, according to the standards ASTM D 664 and EN 14111, respectively. The density at 20 °C was measured under the same conditions as the licuri oil. The flash point determination was carried out according to ASTM D 93 standard, in the Tanaka APM-7 Pensky−Martens closed cup tester. The evaluation of the flow properties, kinematic viscosity, cloud point, pour point, and cold filter plugging point followed the same conditions of the licuri oil. The oxidative stability was determined according to the standard EN 14112 by a Metrohm 743 Rancimat.

2.3. Reduction of the Pd/C Catalyst. Before the reaction, the catalyst reduction step must be performed. In this experiment, the activated carbon-supported palladium catalyst from Sigma-Aldrich was used in a proportion of 5% by mass. Initially, the catalyst underwent a treatment process. The solvents used, *n*-decane (C10) and *n*-dodecane (C12) (99% purity), were supplied by Aldrich.

First, the catalyst was placed in an oven at 105 °C for 12 h for drying. Then, 335 mg of the catalyst was placed in the reactor for the reduction process in 22.4 g of *n*-dodecane.[16]

The reduction of the catalyst, lasting 1 h, occurred after the reactor reached a temperature of 200 °C, with a heating rate of 2 °C min^{-1}. The process occurred under hydrogen gas at a constant flow of 30 mL min^{-1} at ambient pressure under gentle mechanical stirring.

2.4. Semi-Batch Catalytic Deoxygenation Reaction. First, the ideal solvent for the reaction was sought. For this, some factors were evaluated: boiling temperature, vapor pressure, and the retention time in the GC, as some peaks could be overlapped. Of the evaluated solvents, *n*-dodecane was the best suited to the process.[26]

The catalytic deoxygenation reactions were performed in a MicroClave Autoclave Engineers (50 mL) reactor equipped with a Dispersimax impeller (mechanical stirring). The tests were performed at a temperature of 300 °C, at a heating rate of 5 °C min^{-1}. A blank test, in the absence of the catalyst, was carried out, with the objective of evaluating the possibility of thermal deoxygenation at 300 °C.

The process occurred under a constant helium flow of 60 mL min^{-1} with 5% hydrogen, at a pressure of 207 psi. For the pressure to remain high with the gas flow, it was necessary to use a back-pressure regulating valve. The reactions lasted 4 h.

For the start of the reaction, it was necessary to cool the reactor after the reduction step. Thereafter, the mass equivalent to 1.9 mmol for licuri oil or 5.6 mmol for biodiesel was added. The time zero was counted after the reactor reached a temperature of 300 °C, pressure of 207 psi, and a stirring of 1000 rpm, under a 60 mL min^{-1} constant flow of 5% H_2 in He gas mixture.

After the end of the reaction, all of the products were collected, characterized, and weighted to perform the reaction mass balance. The products characterization considered the average of two successful runs.

2.5. Products Characterization. The reactor gas products were analyzed by a Pfeiffer PrismaPlus online quadrupole mass spectrometer (QMS) with closed ion source, heated capillary inlet system, and Quadstar 32-bit software. The H_2 (m/z = 2), He (m/z = 4), CO (m/z = 28), and CO_2 (m/z = 44) signals were uninterruptedly monitored.

The reaction products were analyzed in an HP5890 GC gas chromatograph equipped with a flame ionization detector and an Econo-Cap EC-5 capillary column (30 m length, 0.32 mm diameter, 1.0 μm film thickness). The oven temperature was programmed for a heating rate of 5 °C min^{-1} from 80 to 300 °C. Samples of 0.05 μL were injected at a temperature of 300 °C, with a split rate of 50:1 at 10 psi pressure. The determination of the reaction products concentration was determined using a three-point calibration method for expected products with *n*-decane (C10) as an internal standard.

To evaluate the catalytic deoxygenation reaction, *n*-alkanes yield, *n*-alkanes selectivity, and CO_2 selectivity were calculated according to eqs 4−7. The *n*-alkane yield was calculated by the molar ratio between these compounds and the total reactants (eq 4). The *n*-alkane selectivity was calculated by the percentage ratio between *n*-alkanes yield and the total conversion (eq 5). Conversion is related to the molar ratio between unreacted reactants and the total reactants moles (eq 6). The CO_2 selectivity was calculated from the relationship between the number of CO_2 moles and the number of the total moles of CO and CO_2 gases (eq 7), the possible gaseous co-products for the catalytic deoxygenation reaction

$$n\text{-alkanes yield (\%)} = \frac{n\text{-alkanes moles in product}}{\text{total reactants moles}} \times 100 \quad (4)$$

$$n\text{-alkanes selectivity (\%)} = \frac{n\text{-alkanes yield (\%)}}{\text{conversion (\%)}} \times 100 \quad (5)$$

$$\text{conversion (\%)} = \left\{1 - \left(\frac{\text{unreacted reactants moles}}{\text{total reactants moles}}\right)\right\} \times 100 \quad (6)$$

$$CO_2\ \text{selectivity (\%)} = \frac{\text{moles of } CO_2}{CO + CO_2\ \text{total moles}} \times 100 \quad (7)$$

3. RESULTS AND DISCUSSION

3.1. Licuri Oil Characterization. Table 1 shows the percentages of the fatty acids present in the licuri oil from gas chromatography. The results point out that 81.8% of its molar composition consists of saturated fatty acids and 18.2% of unsaturated fatty acids.

The major compounds are lauric and myristic acids, accounting for more than 50% of the oil composition. Thus, in addition to the other components with chains of 10−18 carbons (excluding the fatty acid C8), the licuri oil presents over 90% of its composition within the range of jet fuel and can

DOI: 10.1021/acsomega.9b01737
ACS Omega 2019, 4, 15849−15855

Table 1. Fatty Acid Composition of Licuri Oil

fatty acid	% experimental results	% literature[21]
caprylic acid (C8:0)	8.8	9.0
capric acid (C10:0)	6.0	6.0
lauric acid (C12:0)	36.0	42.0
myristic acid (C14:0)	16.5	16.0
palmitic acid (C16:0)	8.9	8.0
stearic acid (C18:0)	5.7	4.0
oleic acid (C18:1)	14.2	12.0
linoleic acid (C18:2)	3.9	3.0

be considered as a potential precursor for the production of biofuels.[27] The values of Table 1 agreed with the literature.[21]

The quality of licuri oil was evaluated through the study of its physicochemical characterization. The low acid and iodine values confirm its low unsaturation. The kinematic viscosity was slightly above the result obtained by Teixeira da Silva de La Salles et al.,[21] but quite small compared to other oils, such as soybean and cotton oil, and similar to babassu oil. Table 2 shows the physicochemical properties of the oil, as compared to the literature.[21]

Table 2. Licuri Oil Properties

property	licure oil	
	experimental results	literature[21] results
acid value (mg KOH g^{-1})	0.72	1.4
iodine value (g I_2/100 g)	13.9	18.5
cloud point (°C)	12	
pour point (°C)	9	
cold filter plugging point (°C)	8	
oxidation stability (h)	69.6	
density (kg m^{-3})	924.0	920.0
kinematic viscosity (mm^2 s^{-1})	26.8	23.4

3.2. Licuri Biodiesel Characterization. Table 3 presents the quality parameters of licuri biodiesel. Licuri biodiesel

Table 3. Licuri Biodiesel Properties

property	results obtained	literature[21]	ASTM D 6751	EN 14214
acid value (mg KOH g^{-1})	0.25		0.50	0.50
iodine value (g I_2/100 g)	12.7			120
cloud point (°C)	−2		report	
pour point (°C)	−6			
cold filter plugging point (°C)	−4	−11		
oxidation stability (h)	6.2	8	>3	>8
density (kg m^{-3})	873	876		860−900
kinematic viscosity (mm^2 s^{-1})	3.6	3.8	1.9−6.0	3.5−5.0
flash point (°C)	105		>93	>101
ester content (%)	99.5	98.0		96.5

properties are within the limits specified by the ASTM D 6751 standard. As for the EN 14214 standard, lucuri biodiesel does not meet the oxidative stability specification. However, this parameter can be adjusted with the application of antioxidants. It is also worth mentioning that with its flow properties, and even with a large percentage of saturated chain esters, the licuri biodiesel presented a low cloud point and a low cold filter plugging point.

The catalytic deoxygenation reactions were carried out for licuri oil and licuri biodiesel. The biodiesel displayed an ester content of 99.5%, according to Table 4.

Table 4. Fatty Acid Methyl Esters Composition of Licuri Biodiesel

fatty acid methyl esters	%
C8:0	9.0
C10:0	5.8
C12:0	36.1
C14:0	16.4
C16:0	8.8
C18's	23.4

3.3. Semi-Batch Reactions. Figures 1 and 2 show the catalytic deoxygenation reaction of licuri oil and licuri

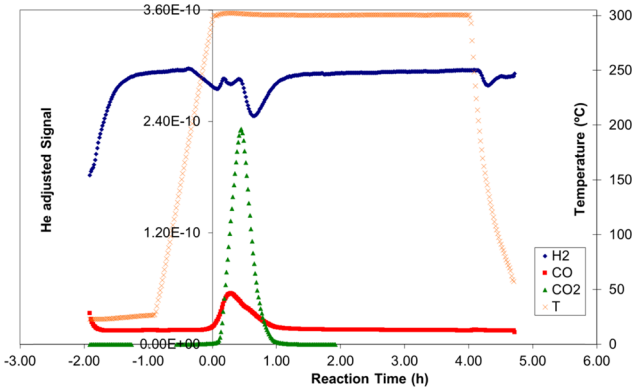

Figure 1. Catalytic semi-batch deoxygenation reaction of licuri oil at 300 °C for 4 h.

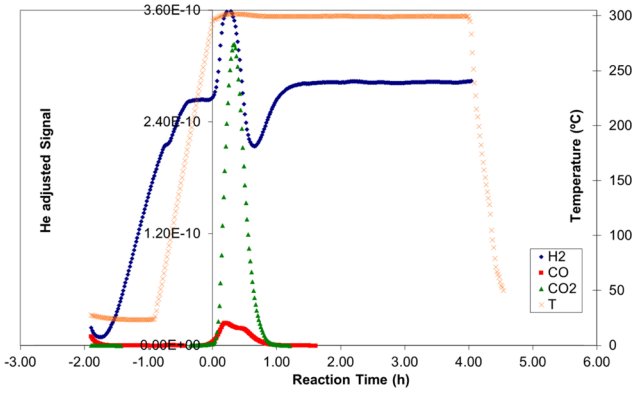

Figure 2. Catalytic semi-batch deoxygenation reaction of licuri biodiesel at 300 °C for 4 h.

biodiesel, respectively. It is possible to verify a greater drop in H_2 concentration at the beginning of the deoxygenation reaction of biodiesel (Figure 2), representing a hydrogen consumption. The temperature line, in turn, remained stable at 300 °C throughout the process, from time zero to the end of the reaction, lasting 4 h.

Licuri oil is composed of different triacylglycerides. Its triacylglyceride structure, because of its three fatty acid chains, has a higher density (very close structure) than biodiesel.

DOI: 10.1021/acsomega.9b01737
ACS Omega 2019, 4, 15849−15855

Indeed, the licuri oil density is 924 kg m^{-3}, compared to 876 kg m^{-3}, for the licuri biodiesel. Thus, it is possible that this causes steric hindrance. It can be a factor for impeding the reaction to occur. On the other hand, the biodiesel structure does not have this inhibiting effect because it contains just one chain. Comparing Figures 1 and 2, it can be noted that the hydrogen consumption for the oil reaction is smaller than that for the biodiesel, indicating a lower reaction rate.

Table 5 indicates the mass balance of the reactions by means of the weighted values for the reactants and products of the reaction. The value of recovery yield was obtained by the mass ratio between the products and the reactants. The product mass is the sum of condensates, the liquid phase in the reactor, solids, and the gaseous products (calculated from the values obtained in the QMS). The overall reactant mass, on the other hand, is the sum of C12 solvent, reactant (oil or biodiesel), and the catalyst, which were weighed and added to the reactor before the beginning of the experiment.

Table 5. Batch Reactions Mass Balance

	reaction precursor	
mass balance	oil	biodiesel
C12 solvent mass (g)	22.425	22.454
reactant (g)	1.326	1.328
catalyst (g)	0.335	0.335
condensed sample (g)	2.716	3.160
reactor remains (g)	19.375	18.513
dry filtrates (g)	0.327	0.331
gaseous products (g)	0.148	0.145
recovery yield (%)	93.7	91.8

The recovery yield of 93.7 wt % for reaction using oil and 91.9 wt % for biodiesel are consistent with this type of batch reactor, in which there is no liquid reactant flow. The losses can be explained mainly by the gaseous products, which were not liquefied in the condenser, besides the adsorption processes, in less quantity.[28] The results were higher than those obtained by Arend et al.,[28] which used a continuous reactor for catalytic deoxygenation of oleic acid, whose mass balance values were below 90% at the steady-state reaction.

Table 6 shows the experimental results of the catalytic deoxygenation reactions, in relation to conversion, *n*-alkanes yield, *n*-alkanes selectivity, and the selectivity of the gas produced in the reaction. It also shows the most probable reaction pathway, and some results from the literature for similar reactions. Conversion is always higher than yield, once byproducts and degraded products from fatty acids are formed, and these oxygenated co-products are not taken into account in the reaction yield. These products are reactants that have been converted but are not part of the yield because these products are not the purpose of the reaction. The final composition of the reaction output is made of *n*-alkanes, oxygenated subproducts, and unconverted reagents.[6]

Table 6. Licuri Deoxygenation Reaction Results at 300 °C

	experimental results				
	licuri oil	licuri biodiesel	stearic acid[7]	stearic acid[29]	bio-oil[29]
conversion (%)	39.6	48.6	62.0	35.2	55.4
n-alkane yield (%)	32.3	39.2	55.8	34.5	32.3
n-alkane selectivity (%)	81.6	80.7	90	98.1	58.3
CO_2 selectivity (%)	76.2	83.4			

All of the literature results presented in Table 6 were obtained in the same conditions of the experimental results of this work, except for bio-oil, which used a Ni/ZrO_2 catalyst.

High CO_2 selectivity values, above 75%, were obtained in both cases. The decarboxylation route (eq 1) is preferred, as the formation of hydrocarbons occurs with the loss of carboxyl, as CO_2. It is known that the formation of unsaturated compounds (eq 2) contributes to the H_2 consumption, competing with the process, leading to the formation, although lower, of carbon monoxide (CO).[26] Carbon monoxide, in this reaction, accelerates the deactivation of the catalyst, decreasing its efficiency over time. Licuri oil composition, on the other hand, presents a lower percentage of unsaturation compared to other oils, such as camelina oil and babassu oil.[30]

Table 6 shows lower values compared to those found for reactions with stearic acid in the literature. However, it is important to note that the feedstock used by Choi et al.[7] and Miao et al.[29] is composed of a single fatty acid component, whose reaction at these conditions is already consolidated, attributed to its higher adsorption on the activated carbon support.[31,32] When the results of the catalytic deoxygenation reactions from licuri oil and biodiesel were compared to the reaction from the bio-oil, whose matrix of components is also complex, the yields and selectivity to *n*-alkanes were higher.[29] These results can also be influenced by the catalyst deactivation since the fixed bed contributes to the deactivation of the catalyst, whose recovery is not possible during the reaction process.[33]

The composition data, in molar percentage, of the *n*-alkanes hydrocarbons obtained for the catalytic deoxydation reaction of both licuri oil and licuri biodiesel are shown in Table 7.

Table 7. Composition of *n*-Alkanes Produced in the Reactions

	reaction precursor	
n-alkane	licuri oil (molar %)	licuri biodiesel (molar %)
C7	8.2	5.2
C9	5.6	4.6
C11	35.1	27.8
C13	16.2	16.6
C15	9.2	10.2
C17	25.7	35.6

According to Ford et al.,[31] the increase of the number of carbons in the chain structure facilitates the catalytic deoxygenation process. It is possible to observe this behavior observing the increase in the concentration for larger hydrocarbon chains and the decrease in the concentration for smaller chains. This point can be discussed, comparing to the reactants chain compositions, in Table 7 (catalytic deoxydation products), with the composition of licuri oil and licuri biodiesel in Tables 1 and 4, respectively. As an example, the increase of C18 composition percentage, from 23.4% in the case of licuri biodiesel (Table 4) to 35.6% C17 in products (Table 7), with the loss of 1 carbon, is observed, after the licuri biodiesel deoxygenation reaction. The C8, in turn, decreased from 9% (Table 4) to 5.2% C7 (Table 7). For the oil, the intensity of the process is less pronounced, probably due to the

DOI: 10.1021/acsomega.9b01737
ACS Omega 2019, 4, 15849−15855

large triacylglyceride structure, making the adsorption process more difficult.

The *n*-alkanes composition of reaction products is very similar to the feedstock (Tables 1, 4, and 7), considering the loss of one carbon in its chain, thus confirming the deoxygenation process, by means of decarboxylation (reaction 1) and/or decarbonylation (reaction 2) and discarding the hydrodeoxygenation (reaction 3), which would lead to a correlation without carbon loss in the chain. This is ratified by the formation and release of monoxide and dioxide carbon gas. Therefore, for the reaction under these conditions, the occurrence of the decarboxylation pathway is suggested since the selectivity to CO_2 is much greater than that to CO, remembering that the sum of these selectivities is always 100%.

4. CONCLUSIONS

The attainment of an *n*-alkane conversion up to 39.2% in the present wok can be considered satisfactory since the reaction in this experiment occurs in a semi-batch reaction with fixed-bed reactor. This fact confirms the potential of licuri biodiesel as a precursor feedstock for biojet fuel. Despite the high cost, the Pd/C catalyst can present better results, if it is applied in continuous bed.

However, it is important to note that the product of this research is not ready be used once the *n*-alkanes require the isomerization step followed by the separation process by fractional distillation. The isomerization step is needed, as these hydrocarbons must be converted into short iso-alkanes, which are compounds with superior cold flow properties. Therefore, it is possible to meet the strict jet fuel requirements, according to ASTM D 1655 standard for jet fuel certification and to ASTM D 7566 for fuels containing alternative synthesized hydrocarbons.[34,35]

In this work, a yield of 32.3% for *n*-alkanes was obtained for the licuri oil, a result close to the one for biodiesel. This result, besides the selectivity to alkanes, suggests that the trans-esterification process of the biodiesel synthesis is not an outstanding stage for the optimization for the biojet production process. However, the decrease of the selectivity to CO_2 when using the oil in the place of biodiesel indicates the possibility of shortening the useful life of the catalyst because CO deactivates the catalyst very strongly.[26]

AUTHOR INFORMATION

Corresponding Author

*E-mail: natalyjp@gmail.com. Tel: +55 83 3216-7441.

ORCID

Ary S. Maia: 0000-0002-5930-790X

Nataly A. Santos: 0000-0003-0001-5192

Notes

The authors declare no competing financial interest.

ACKNOWLEDGMENTS

This study was partly financed by Conselho Nacional de Desenvolvimento Científico e Tecnológico—Brasil (CNPq) and Coordenação de Aperfeiçoamento de Pessoal de Nível Superior—Brasil (CAPES)—Finance Code 001. The authors thank Dr. Lamb from the Department of Chemical and Biomolecular Engineering, North Carolina State University, for his assistance and laboratory structure and support for research.

REFERENCES

(1) Cortez, L. A. B.; Nigro, F. E. B.; Nogueira, F. A. H.; et al. Perspectives for Sustainable Aviation Biofuels in Brazil. *Int. J. Aerosp. Eng.* **2015**, No. 264898.

(2) Li, X.; Mupondwa, E.; Tabil, L. Technoeconomic analysis of biojet fuel production from camelina at commercial scale: Case of Canadian Prairies. *Bioresour. Technol.* **2018**, *249*, 196−205.

(3) Mohd Yunos, S. N. M.; Abdul Ghafir, M. F.; Wahab, A. A. Evaluation on alternative jet fuels application and their impact on airport environmental charges. *J. Eng. Appl. Sci.* **2016**, *11*, 7380−7387.

(4) Ford, J. P.; Thapaliya, N.; Kelly, M. J.; Roberts, W. L.; Lamb, H. H. Semi-Batch Deoxygenation of Canola- and Lard-Derived Fatty Acids to Diesel-Range Hydrocarbons. *Energy Fuels* **2013**, *27*, 7489−7496.

(5) Zhang, Y.; Bi, P.; Wang, J.; Jiang, P.; Wu, X.; Xue, H.; Liu, J.; Zhou, X.; Li, Q. Production of jet and diesel biofuels from renewable lignocellulosic biomass. *Appl. Energy* **2015**, *150*, 128−137.

(6) Shahinuzzaman, M.; Yaakob, Z.; Ahmed, Y. Non-sulphide zeolite catalyst for bio-jet-fuel conversion. *Renewable Sustainable Energy Rev.* **2017**, *77*, 1375−1384.

(7) Choi, I. H.; Lee, J. S.; Kim, C. U.; et al. Production of bio-jet fuel range alkanes from catalytic deoxygenation of Jatropha fatty acids on a $WO_x/Pt/TiO_2$ catalyst. *Fuel* **2018**, *215*, 675−685.

(8) Pattanaik, B. P.; Misra, R. D. Effect of reaction pathway and operating parameters on the deoxygenation of vegetable oils to produce diesel range hydrocarbon fuels: A review. *Renewable Sustainable Energy Rev.* **2017**, *73*, 545−557.

(9) Wang, W.-C.; Tao, L. Review of bio-jet fuel conversion technologies. *Renewable Sustainable Energy Rev.* **2016**, *53*, 801−822.

(10) National Academies of Sciences, Engineering, and Medicine (NASEM). *Commercial Aircraft Propulsion and Energy Systems Research: Reducing Global Carbon Emissions*; The National Academies Press: Washington, DC, 2016.

(11) Choi, I. H.; Hwang, K. R.; Choi, H. Y.; et al. Catalytic deoxygenation of waste soybean oil over hybrid catalyst for production of bio-jet fuel: in situ supply of hydrogen by aqueous-phase reforming (APR) of glycerol. *Res. Chem. Intermed.* **2018**, *44*, 3713−3722.

(12) Asikin-Mijan, N.; Lee, H. V.; Juan, J. C.; Noorsaadah, A. R.; Taufiq-Yap, A. R. Catalytic deoxygenation of triglycerides to green diesel over modified CaO-based catalysts. *RSC Adv.* **2017**, *7*, 46445−46460.

(13) Silva, F. C. M.; Lima, M. S.; Costa Neto, C. O.; et al. Catalytic deoxygenation of C18 fatty acids over HAlMCM-41 molecular sieve. *Biomass Convers. Biorefin.* **2018**, *8*, 159−167.

(14) Pongsiriyakul, K.; Kiatkittipong, W.; Kiatkittipong, K.; Laosiripojana, N.; Faungnawakij, K.; Adhikari, S.; Assabumrungrat, S. Alternative Hydrocarbon Biofuel Production via Hydrotreating under a Synthesis Gas Atmosphere. *Energy Fuels* **2017**, *31*, 12256−12262.

(15) Snåre, M.; Kubičková, I.; Mäki-Arvela, P.; Eränen, K.; Murzin, D. Y. Heterogeneous catalytic deoxygenation of stearic acid for production of biodiesel. *Ind. Eng. Chem. Res.* **2006**, *45*, 5708−5715.

(16) Arora, P.; Greenfelt, E. L.; Olsson, L.; Creaser, D. Kinetic study of hydrodeoxygenation of stearic acid as model compound for renewable oils. *Chem. Eng. J.* **2019**, *364*, 376−389.

(17) Kubička, D.; Horáček, J.; Setnička, M.; Bulánek, R.; Zukal, A.; Kubičková, I. Effect of Support-Active Phase Interactions on the Catalyst Activity and Selectivity in Deoxygenation of Triglycerides. *Appl. Catal., B* **2014**, *145*, 101−107.

(18) Simakova, I.; Simakova, O.; Maki-Arvela, P.; Simakov, A.; Estrada, M.; Murzin, D. Y. Deoxygenation of Palmitic and Stearic Acid Over Supported Pd Catalysts: Effect of Metal Dispersion. *Appl. Catal., A* **2009**, *355*, 100−108.

(19) Mäki-Arvela, P.; Kubickova, I.; Snåre, M.; Eränen, K.; Murzin, D. Y. Catalytic deoxygenation of fatty acids and their derivatives. *Energy Fuels* **2007**, *21*, 30−41.

DOI: 10.1021/acsomega.9b01737
ACS Omega 2019, 4, 15849−15855

(20) Wang, W.-C.; Thapaliya, N.; Campos, A.; Stikeleather, L.; Roberts, W. Hydrocarbon fuels from vegetable oils via hydrolysis and thermo-catalytic decarboxylation. *Fuel* **2012**, *95*, 622−629.
(21) Teixeira da Silva de La Salles, K.; Meneghetti, S. M. P.; Ferreira de La Salles, W.; et al. Characterization of *Syagrus coronata* (Mart.) Becc. oil and properties of methyl esters for use as biodiesel. *Ind. Crops Prod.* **2010**, *32*, 518−521.
(22) Crepaldi, I. C.; De Almeida-Muradian, L. B.; Rios, M. G. D.; Penteado, M. D. V. C.; Salatino, A. Composição nutricional do fruto de licuri (*Syagrus coronata* (Martius) Beccari). *Rev. Bras. Bot.* **2001**, *24*, 155−159.
(23) Hartman, L.; Lago, R. C. Rapid preparation of fatty acid methyl ester from lipids. *Lab Pract.* **1973**, *22*, 475−476.
(24) Zzopardi, L. M. *Official Methods and Recommended Practices of the American Oil Chemists' Society*, 7th ed.; AOCS: Urbana, IL, 2017.
(25) Santos, N. A.; Damasceno, S. S.; Araújo, P. H. M.; Marques, V. C.; Rosenhaim, R.; Fernandes, V. J., Jr.; Queiroz, N.; Santos, I. M. G.; Maia, A. S.; Souza, A. G. Caffeic acid: an efficient antioxidant for soybean biodiesel contaminated with metals. *Energy Fuels* **2011**, *25*, 4190−4194.
(26) Immer, J. G.; Kelly, M. J.; Lamb, H. H. Catalytic reaction pathways in liquid-phase deoxygenation of C18 free fatty acids. *Appl. Catal., A* **2010**, *375*, 134−139.
(27) Jiménez-Díaz, L.; Caballero, A.; Pérez-Hernández, N.; Segura, A. Microbial alkane production for jet fuel industry: motivation, state of the art and perspectives. *Microb. Biotechnol.* **2017**, *10*, 103−124.
(28) Arend, M.; Nonnen, T.; Hoelderich, W. F.; Fischer, J.; Groos, J. Catalytic deoxygenation of oleic acid in continuous gas flow for the production of diesel-like hydrocarbons. *Appl. Catal., A* **2011**, *399*, 198−204.
(29) Miao, C.; Marin-Flores, O.; Dong, T.; Gao, D.; Wang, Y.; Garcia-Pérez, M.; Chen, S. Hydrothermal Catalytic Deoxygenation of Fatty Acid and Bio-oil with In Situ H_2. *ACS Sustainable Chem. Eng.* **2018**, *6*, 4521−4530.
(30) Llamas, A.; Al-Lal, A. M.; Hernandez, M.; Lapuerta, M.; Canoira, L. Biokerosene from Babassu and Camelina Oils: Production and Properties of Their Blends with Fossil Kerosene. *Energy Fuels* **2012**, *26*, 5968−5976.
(31) Ford, J. P.; Immer, J. G.; Lamb, H. H. Palladium Catalysts for Fatty Acid Deoxygenation: Influence of the Support and Fatty Acid Chain Length on Decarboxylation Kinetics. *Top Catal.* **2012**, *55*, 175−184.
(32) Yang, C.; Nie, R.; Fu, J.; Hou, Z.; Lu, X. Production of aviation fuel via catalytic hydrothermal decarboxylation of fatty acids in microalgae oil. *Bioresour. Technol.* **2013**, *146*, 569−573.
(33) Hermida, L.; Abdullah, A. Z.; Mohamed, A. R. Deoxygenation of fatty acid to produce diesel-like hydrocarbons: A review of process conditions, reaction kinetics and mechanism. *Renewable Sustainable Energy Rev.* **2015**, *42*, 1223−1233.
(34) Santillan-Jimenez, E.; Crocker, M. Catalytic deoxygenation of fatty acids and their derivatives to hydrocarbon fuels via decarboxylation/decarbonylation. *J. Chem. Technol. Biotechnol.* **2012**, *87*, 1041−1050.
(35) Vozka, P.; Vrtiška, D.; Šimáček, P.; Kilaz, G. Impact of Alternative Fuel Blending Components on Fuel Composition and Properties in Blends with Jet A. *Energy Fuels* **2019**, *33*, 3275−3289.

DOI: 10.1021/acsomega.9b01737
ACS Omega 2019, 4, 15849−15855